

## Introduction

Blackbodies are commonly used as a transfer medium in the calibration of radiation thermometers. The ideal blackbody is perfectly isothermal and has an emissivity of precisely 1 at all wavelengths. However, no real material has an emissivity as high as 1, so practical blackbodies are created by forming a cavity, made to be as isothermal as possible, inside a material with a relatively high *intrinsic emissivity* (~0.9). These cavities take advantage of multiple internal reflections to provide an *effective emissivity* very close to 1 (~0.995 or higher). A radiation thermometer can then view the approximately-blackbody radiation emerging through an aperture at the front of the cavity.

In general, the *local effective emissivity* of a blackbody cavity varies at each point along the inside of the cavity walls, and depends largely on the intrinsic emissivity of the cavity material and the geometry of the cavity. When a radiation thermometer views the inside of a blackbody cavity, the effective emissivity that it sees is a weighted average of the local effective emissivities of the cavity walls within the thermometer's field of view. This *integrated emissivity* will vary from thermometer to thermometer, and will vary for a single thermometer if its focal point is changed – for example, by moving the thermometer so that it is focused either on the cavity aperture or on the cavity base.

The local effective emissivity of the cavity walls is also affected by any temperature non-uniformities along the length of the cavity. Often, the front of the cavity is cooler than the base due to heat loss through the aperture. This effect causes the local effective emissivity to become dependent on wavelength, and thus the integrated emissivity for a given radiation thermometer will depend on its operating wavelength and bandwidth.

In order to properly calibrate a radiation thermometer, it is essential that the integrated emissivity of the cavity is known for the device under calibration (DUC). When a radiation thermometer is also used as the reference device (REF), it is also essential that the integrated emissivity is known for the REF, as the integrated emissivities for the two devices will differ if the DUC and REF have different fields of view or operate at different wavelengths.

The purpose of this technical guide is to provide advice on how to calculate the integrated emissivity for any cavity/thermometer combination. If high accuracy is not required, and if the cavity is approximately isothermal, then a simple formula can be used to determine the integrated emissivity. However, for high accuracy, methods for calculating the integrated emissivity are highly mathematical and require iterative algorithms to achieve a solution. Hence, this technical guide is accompanied by a software application that implements algorithms to calculate

both the local effective emissivity at all points on the inside of a cavity and the integrated emissivity for a radiation thermometer viewing the cavity. Instructions for using the software are included in this technical guide, and for those readers interested, the mathematical details are given in the appendices.

## Blackbody Radiation

The radiation emitted by an ideal blackbody is described by Planck's law for spectral radiance, as a function of temperature  $T$  and wavelength  $\lambda$ :

$$L_b(\lambda, T) = \frac{c_1}{\lambda^5 \left[ \exp\left(\frac{c_2}{\lambda T}\right) - 1 \right]}, \quad (1)$$

where the units of  $T$  are kelvin, and  $c_1$  and  $c_2$  are known as the first and second radiation constants, respectively, and have values  $c_1 = 1.191\,042\,82 \times 10^{-16} \text{ W m}^2$  and  $c_2 = 0.014\,388 \text{ m K}$ . The subscript  $b$  on the symbol  $L$  indicates that the spectral radiance is that of an ideal blackbody.

In general, the cavities used for radiation thermometer calibrations are not ideal blackbodies, but have an effective emissivities somewhat less than 1 and exhibit some degree of temperature non-uniformity. Thus, each point inside the cavity will have a spectral radiance given by

$$L(\lambda) = \varepsilon_{\text{eff}} L_b(\lambda, T_0), \quad (2)$$

where  $\varepsilon_{\text{eff}}$  is the local effective emissivity at that point of the cavity, and  $T_0$  can be arbitrarily defined as the temperature at the centre of the base of the cavity. Note that  $\varepsilon_{\text{eff}}$  will depend on the geometry of the cavity, the intrinsic emissivity at each point in the cavity, and the temperature distribution within the cavity. Also note that the local effective emissivity at any point inside the cavity may be greater than 1 if the temperature of that point is higher than  $T_0$ .

## Radiation Thermometer Signal

When a radiation thermometer views a cavity, the signal produced is equal to the integral of equation (2) over the thermometer's spectral responsivity,  $R(\lambda)$ , and over the thermometer's field of view, resulting in:

$$\begin{aligned} S(T) &= \varepsilon_{\text{bb}} \int_0^\infty R(\lambda) L_b(\lambda, T_0) d\lambda \\ &= \varepsilon_{\text{bb}} S(T_0), \end{aligned} \quad (3)$$



**Figure 1.** The field of view of a radiation thermometer is separated into an umbral region (dark shading) and a penumbral region (light shading). All the rays from the cavity surface within the umbral region that pass through the measurement spot at the focal plane are detected, but only some of those rays within the penumbral region are detected.

where  $\epsilon_{bb}$  is the integrated emissivity of the cavity/thermometer combination and  $T$  is the temperature that would be inferred by the thermometer in the absence of any other effects (such as ambient effects and the size-of-source effect; see [1, 2] for a discussion of these). In equation (3), it has been assumed that the value of  $\epsilon_{eff}$  at each point in the cavity does not vary over the wavelength range covered by the thermometer's spectral responsivity. The value of the integrated emissivity,  $\epsilon_{bb}$ , then depends on the distribution of local effective emissivity values within the field of view of the thermometer.

The field of view of a typical radiation thermometer, illustrated in Figure 1, comprises two zones: a zone that is fully seen by the detector (the umbral region), and a zone that is only partially seen by the detector (the penumbral, or partially-vignetted, region). The locations of these two regions are determined by two apertures within the optical system of the thermometer, and by the focal length of the optical system. The two apertures are referred to as the *aperture stop* and the *field stop*. The aperture stop (equivalent to the f-stop in a camera) determines the solid angle of rays that are detected by the thermometer, and the field stop determines the size of the measurement spot at the focal plane. For focusable radiation thermometers, the aperture stop should sit behind the lens (as shown in Figure 1), but for fixed-focus instruments, the aperture stop may coincide with the lens holder or may be positioned in front of the lens.

To determine the locations of the umbral and penumbral regions, we define an 'apparent' aperture stop to be the projection of the actual aperture stop through the optical system, and this defines the plane from which the working distance (focal distance) is measured (see Figure 1). Note that when the aperture stop coincides with the lens holder or is in front of the optical system, then the apparent aperture stop is identical to the real aperture stop.

The umbral and penumbral regions are determined by extending the four lines from the top and bottom of the apparent aperture stop to each of the top and bottom of the measurement spot, at the focal plane, onto the surface of the cavity. In Figure 1 the umbral and penumbral regions are shown by the darker and lighter shadings, respectively. As drawn, the focal plane is at the opening of the cavity, but by moving the thermometer relative to the cavity, the focal plane can be positioned at any location. Any ray from within the umbral region on the cavity surface that passes through the measurement spot (or can be back-projected through the measurement spot if the cavity surface is closer than the focal distance) intersects

the apparent aperture stop, and is thus detected. However, only some of the rays from within the penumbral region that pass through the measurement spot will intersect the apparent aperture stop, and this fraction decreases towards the outer part of the penumbral region. Beyond the penumbral region, none of the rays that pass through the measurement spot intersect the apparent aperture stop, and so none are detected.

The software associated with this Technical Guide automatically determines the locations of the umbral and penumbral regions and calculates the value of  $\epsilon_{bb}$  accordingly.

## Calculating the Local Effective Emissivity

Several methods have been developed for calculating the local effective emissivity,  $\epsilon_{eff}$ , of blackbody cavities. The method used in this Technical Guide and the associated software is that of Bedford and Ma [3, 4], which is based on the solution of a set of integral equations describing the radiation exchange between each surface inside the cavity. The method uses the zonal approximation of heat transfer, where each surface is divided into a large number of small regions within which the local effective emissivity is assumed to be constant. This allows the integrals to be replaced by sums, leading to a simple but accurate numerical solution of a set of simultaneous analytical equations.

The details of these calculations are given in Appendix A.

## Calculating the Integrated Emissivity

The integrated emissivity,  $\epsilon_{bb}$ , is calculated as the ratio of the flux reaching the apparent aperture stop (and hence the detector) of the radiation thermometer from the cavity surface to the flux that would reach the apparent aperture stop from an identical cavity with an intrinsic surface emissivity of 1. This equates to a weighted average of the local effective emissivities within the field of view of the radiation thermometer, where the weights depend on geometry of the cavity, the distance from the cavity surface to the apparent aperture stop, and whether each part of the field of view is within the umbral or the penumbral region.

The details of these calculations are given in Appendix B.

## Approximate Emissivity Formulae

In some instances, the high accuracy obtainable using the calculations described above, which are implemented in the accompanying software, is not required, and a simple 'ball-park' estimate may suffice.

### Cylindrical Cavity

If it can be assumed that the cavity is reasonably isothermal, and if the intrinsic emissivity of all the internal surfaces is the same, with a value of  $\epsilon_s$ , then for a cylindrical cavity with a flat or conical base, the integrated emissivity is approximately given by [5]

$$\epsilon_{bb} \approx 1 - (1 - \epsilon_s) \left( \frac{R_{\text{aper}}}{L} \right)^2, \quad (4)$$

where  $R_{\text{aper}}$  is the radius of the aperture at the front of the cavity, and  $L$  is the total length of the cavity. This approximation breaks down when the ratio of  $R_{\text{aper}}$  to  $L$  is large, or when the emissivity,  $\epsilon_s$ , is low.

### Spherical Cavity

For an isothermal spherical cavity of diameter  $D$ , with a circular aperture of radius  $R_{\text{aper}}$ , the local effective emissivity is independent of position on the cavity wall, and thus the integrated emissivity is equal to the local effective emissivity at any point. This is given by [6]

$$\epsilon_{bb} = \frac{\epsilon_s}{1 - \frac{(1 - \epsilon_s)}{2} \left[ 1 + \sqrt{1 - \left( \frac{2R_{\text{aper}}}{D} \right)^2} \right]}. \quad (5)$$

When  $R_{\text{aper}}$  is small compared to  $D$ , and when  $\epsilon_s$  is relatively high (close to 1), the integrated emissivity for a spherical cavity is identical to equation (4), but with  $L$  replaced by  $D$ :

$$\epsilon_{bb} \approx 1 - (1 - \epsilon_s) \left( \frac{R_{\text{aper}}}{D} \right)^2. \quad (6)$$

## The Blackbody Emissivity Software

The *Blackbody Emissivity* software is designed to calculate the local effective emissivities of cylindro-conical cavities (possibly including a lid containing an aperture), and the integrated emissivity for a radiation thermometer viewing the cavity. The software interface provides graphical information as well as numerical values. Files may be saved using the extension .ebb.

The graphical interface is shown in Figure 2. The screen is split into four panels, whose widths and heights can be changed by dragging the intersecting borders. On the left is a panel called *Emissivity Data*, which is a numerical spreadsheet containing the results of the local effective emissivity calculations. In the centre is a panel called *Emissivity Graph*, which contains a graph of the data in the *Emissivity Data* panel. The panel on the right, called *Parameters*, gives a summary of the cavity parameters and the results of the integrated emissivity calculation. Finally, the lower panel, called *Cavity Schematic*, displays a drawing of the cavity and a representation of the radiation thermometer viewing the cavity, including rays defining the field of view. The two parts of this schematic are drawn once valid cavity and thermometer parameters have been entered. Note that all surfaces within the cavity are assumed to be isotropically diffuse (i.e., their emittance and reflectance properties are independent of angle). The schematic can be chosen to be drawn so that the shade of grey of each surface is proportional to the intrinsic emissivity of that surface ( $\epsilon=0$  = white,  $\epsilon=1$  = black), through the *Cavity|Use Emissivity Shading* menu.

### Entering the Cavity Geometry

The geometry of the cavity can be entered either by choosing the *Cavity|Calculate Effective Emissivity (Eeff)* menu or by clicking on the *Eeff* button on the tool bar. This brings up the dialog box shown in Figure 3. There are three general geometries that the

software can handle, as shown in Figure 4, all of which may or may not contain a lid with an aperture. These are: (a) a cylinder; (b) a cone; and (c) a cylinder with a conical base. For the case in Figure 4(a), a hole may be designed into the base for the purpose of calculating the reflectance of a sample placed over the hole. All geometries are assumed to be axially symmetric. As valid combinations of the cavity geometry are entered, a schematic of the cavity is drawn, or updated, in the *Cavity Schematic* panel.

The check boxes in the *Cavity Geometry* group box are used to select the type of geometry. These selections are not all independent and the software prevents invalid combinations from being selected. These selections also determine which additional information needs to be entered. Selecting the *No wall* check box specifies the conical geometry shown in Figure 4(b).

*Cavity Dimensions* group box: here the cavity *Length* and cavity *Diameter* are specified. The cavity length,  $L_{cav}$ , refers to the length of just the cylindrical section of the cavity (not including the conical section). The cavity diameter,  $D_{cav}$ , is either the diameter of the cylindrical section, or the diameter of the mouth of the cone when there is no cylindrical section (i.e., when the *No wall* check box is selected).

*Hole or Cone* group box: the information entered here depends on whether a conical section has been included in the geometry and whether a hole has been included in the cylindrical base. For a conical section, either the *cone Length* or the *cone angle* must be entered, and the quantity not entered is automatically calculated once a valid cavity diameter has been entered. The cone length,  $L_{cone}$ , is the length of the cone along its central axis (not the sloping length), and the cone angle,  $\theta$ , is the full angle of the apex. The *cone Emissivity* is the intrinsic emissivity of the inner surface of the cone. For a cavity without a conical section but with a hole in the base, the *hole Diameter* and *Sample reflectance* must be entered. The sample reflectance is the reflectance of the sample placed over the hole.

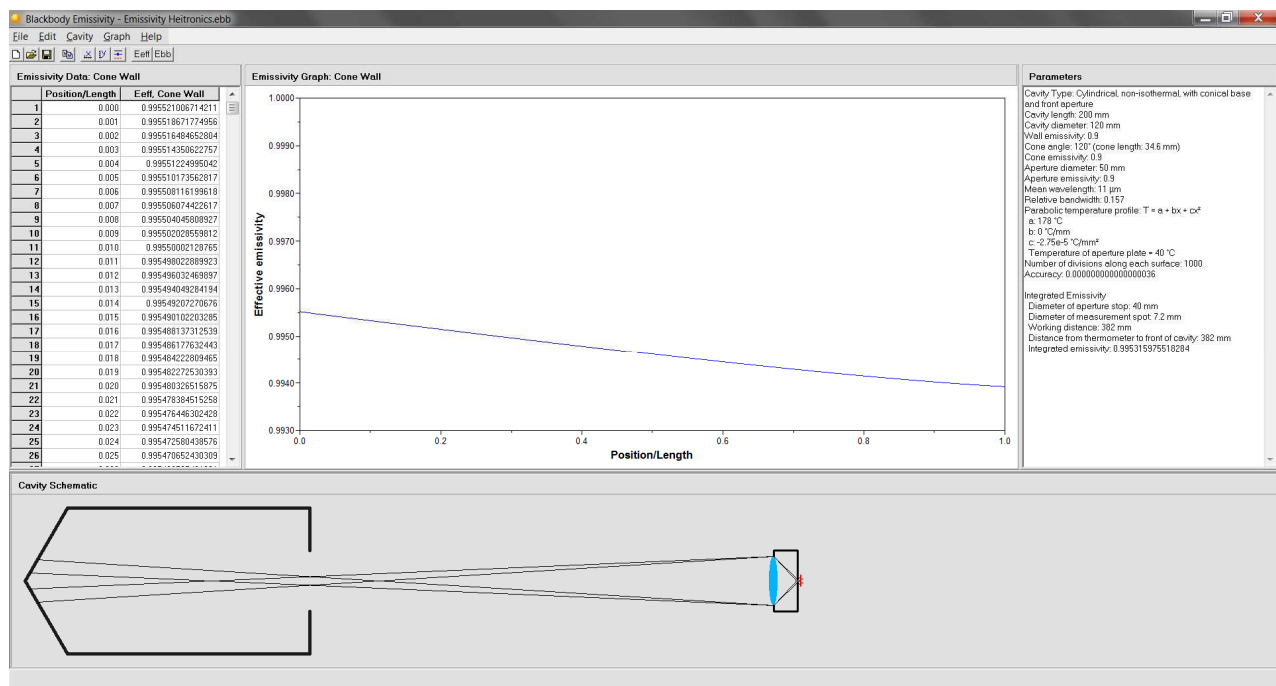


Figure 2. Graphical interface for the *Blackbody Emissivity* software, showing the *Emissivity Data*, *Emissivity Graph*, *Parameters*, and *Cavity Schematic* panels.

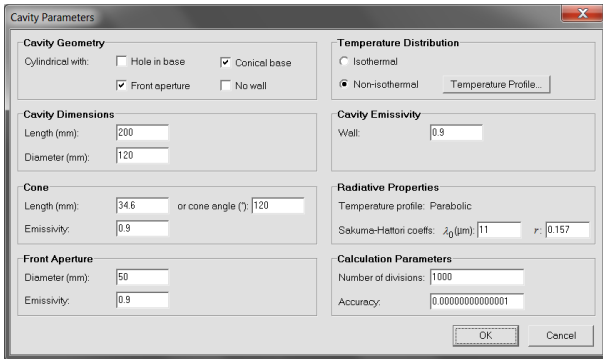
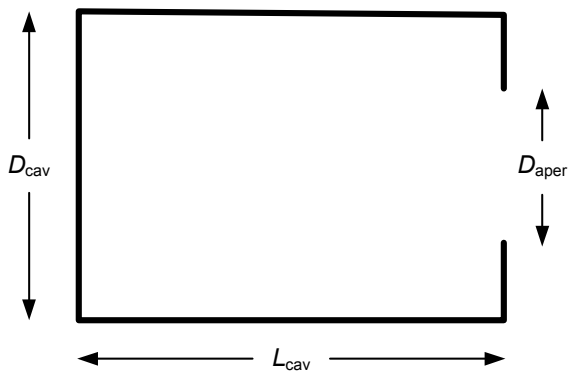
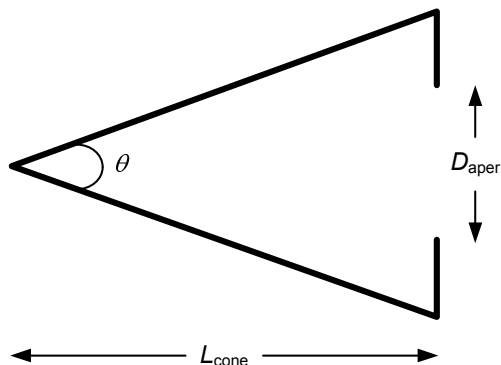


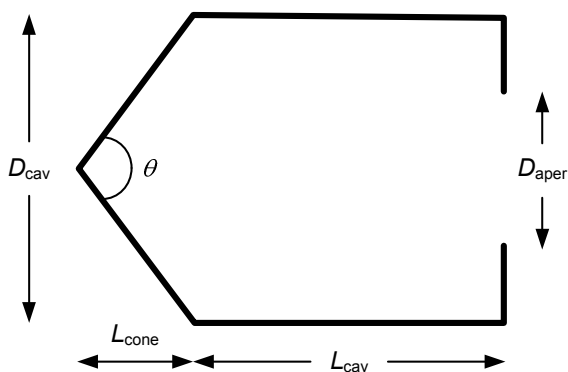
Figure 3. Dialog box for entering the cavity geometry.



(a) Cylinder



(b) Cone



(c) Cylinder with conical base (cylindro-cone)

Figure 4. The three geometries handled by the software. Each may be designed with or without the lid containing the aperture.

Front Aperture group box: when a lid with an aperture is included in the geometry (i.e., when the Front aperture check box is selected), the Diameter of the aperture,  $D_{\text{aper}}$ , and the intrinsic Emissivity of the lid's inner surface must be specified.

Cavity Emissivity group box: here the emissivities of the Wall and Base are entered. The wall emissivity is the intrinsic emissivity of the wall of the cylindrical part of the cavity, and the base emissivity is the intrinsic emissivity of the flat base of the cylindrical cavity when a cone has not been included in the geometry.

### Entering the Cavity Temperature Distribution

The same dialog box allows the cavity to be specified as either Isothermal or Non-isothermal in the Temperature Distribution group box. For non-isothermal cavities, a temperature distribution must be entered by clicking on the Temperature Profile button. Clicking this button brings up the dialog box shown in Figure 5. The Temperature Profile group box allows one of three different temperature profiles to be chosen: (i) Linear; (ii) Constant/Linear; or (iii) Parabolic.

For the linear profile, two parameters are required in the Linear Parameters group box:  $T$  at centre of base and  $T$  at front of cavity. The temperature at the centre of the base refers to either the temperature at the centre of a flat base for a cylindrical cavity, or the temperature at the apex of the cone for cavities including a conical section. The temperature at the front of the cavity is the temperature of the wall at the cavity mouth. Temperatures in between are linearly interpolated in the direction of the cavity axis.

For the constant/linear profile, the same two parameters as for the linear profile are required to be entered in the Constant/Linear Parameters group box, and, additionally, a third parameter Constant from centre of base to  $x =$  must also be entered. This third parameter specifies the distance from the base, or apex of the cone, up to which the temperature is constant, after which it changes linearly along the cavity-axis direction to the temperature specified at the front of the cavity.

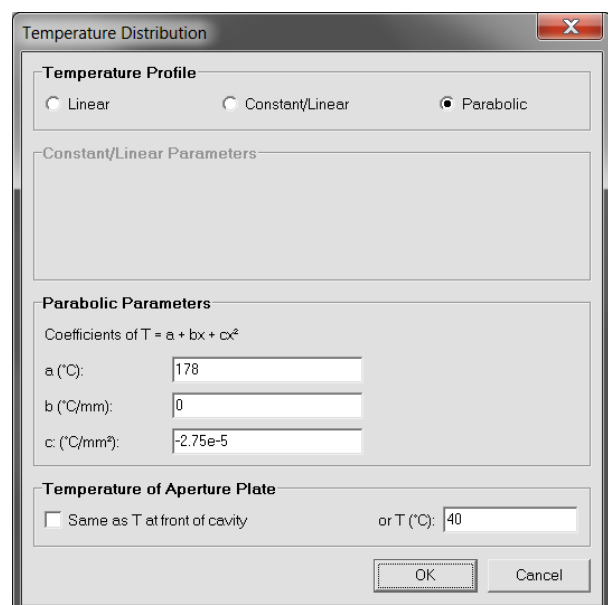


Figure 5. Dialog box for entering the temperature distribution along the axis of the cavity, with a parabolic profile selected.

For the parabolic profile, three parameters are required in the `Parabolic Parameters` group box. These are the parameters  $a$ ,  $b$ , and  $c$  of the quadratic equation  $T = a + bx + cx^2$ , where  $x = 0$  corresponds to the base of the cavity or apex of the cone, and  $x$  increases towards the front of the cavity where  $x = L_{\text{cone}} + L_{\text{cav}}$ .

When the cavity includes a lid with an aperture, the temperature of the aperture plate can be specified to be with the Same as T at front of cavity or some other specified temperature, in the `Temperature of Aperture Plate` group box.

#### Determining the Radiative Properties

When the temperature distribution is non-isothermal, the local effective emissivities along the cavity surfaces will depend on the relative spectral responsivity of the radiation thermometer viewing the cavity. The relative spectral responsivity must be specified in the `Radiative Properties` group box in the `Cavity Parameters` dialog box shown in Figure 3 (the selected temperature profile is also displayed here). The relative spectral responsivity is characterised in terms of its Sakuma–Hattori coefficients, where the signal for a finite-bandwidth radiation thermometer is approximated by the Sakuma–Hattori equation,

$$S(T) = \frac{C}{\exp\left(\frac{c_2}{AT+B}\right) - 1}, \quad (7)$$

where the coefficients  $A$  and  $B$  are related to the mean wavelength,  $\lambda_0$ , and standard deviation,  $\sigma$ , of the spectral responsivity, such that [7]

$$A = \lambda_0(1 - 6r^2) \quad (8)$$

and

$$B = \frac{c_2}{2} r^2, \quad (9)$$

where the relative bandwidth,  $r$ , is given by

$$r = \frac{\sigma}{\lambda_0}. \quad (10)$$

The software requires values of  $\lambda_0$  and  $r$  to be entered. These can be determined from  $A$  and  $B$  as

$$\lambda_0 = \frac{c_2 A}{c_2 - 12B} \quad (11)$$

and

$$r = \sqrt{\frac{2B}{c_2}}. \quad (12)$$

**Example 1:** in the monochromatic approximation  $B = 0$ , so in this case  $\lambda_0 = A$  (= operating wavelength) and  $r = 0$ .

**Example 2:** for a broadband spectral responsivity, whose shape can be approximated as rectangular (often specified by a wavelength range),

$$A = \lambda_0 \left(1 - \frac{\Delta\lambda^2}{2\lambda_0^2}\right) \quad (13)$$

and

$$B = \frac{c_2 \Delta\lambda^2}{24\lambda_0^2}, \quad (14)$$

where  $\lambda_0$  is the centre wavelength of the range and  $\Delta\lambda$  is the width of the wavelength range. Substituting equation (14) into equation (12) gives

$$r = \frac{\Delta\lambda}{\sqrt{12}\lambda_0}. \quad (15)$$

Thus, for an IR thermometer operating over the 8–14  $\mu\text{m}$  range, where  $\lambda_0 = 11 \mu\text{m}$  and  $\Delta\lambda = 6 \mu\text{m}$ , equation (15) gives  $r = 0.157$ .

#### Entering the Calculation Parameters

The `Calculation Parameters` group box in Figure 3 requires two values to be entered: the `Number of divisions` that each surface (the cylinder wall, half the cylinder base, the cone wall, and half the aperture plate) is divided into when performing the calculations for the local effective emissivity, and the `Accuracy` for the calculations. The software will continue iterating until the largest change in all the local effective emissivity values, from one iteration to the next, is less than the accuracy value. The `Number of divisions` and `Accuracy` are stored as default values and any changes become new default values.

#### Calculating the Local Effective Emissivity

Once the cavity parameters have been entered, clicking the `OK` button in the `Cavity Parameters` dialog box in Figure 3 causes the calculations to begin. Progress through the iterations is displayed in the status bar at the bottom of the main window. Once started, the calculations can be aborted if necessary by clicking on the `Stop` button that appears on the right-hand side of the status bar. Upon completion of the calculations (or if the calculations are aborted), the `Emissivity Data`, `Emissivity Graph`, and `Parameters` panels are filled appropriately.

#### Local Effective Emissivity Graph

The graph plotted in the `Emissivity Graph` panel is a plot of the local effective emissivity along one surface of the cavity. Each individual surface can be selected from the `Graph` menu. The currently plotted surface is displayed at the top of the panel. The  $x$ -axis for each surface ranges from 0 to 1 and represents a relative distance. For the conical section,  $x = 0$  corresponds to the apex of the cone and  $x = 1$  to the top or bottom of the cone (the local effective emissivity along the cavity surfaces is symmetrical with respect to the cavity axis). For a cavity with a flat base,  $x = 0$  corresponds to the centre of the base and  $x = 1$  to the intersection of the base with the cylindrical wall. For the cylindrical wall section,  $x = 0$  corresponds to the left-hand end of the wall and  $x = 1$  to the right-hand end. Finally, for a cavity with a lid containing an aperture,  $x = 0$  corresponds to the point on the lid adjacent to the top or bottom of the aperture and  $x = 1$  to the intersection of the lid with the cylindrical wall or mouth of the cone.

These designations can be viewed in the software by holding the mouse over the heading above the graph.

The axes on the graph can be scaled via the `Graph|x-Axis` and `Graph|y-Axis` menu (see Figure 6), and the style and colour of the plotted line can be changed via the `Graph|Line Style` menu (see Figure 7). Additionally, the graph can be copied to the clipboard or printed. Graph styles can be saved to disk or saved as the default style through the `Graph` menu.

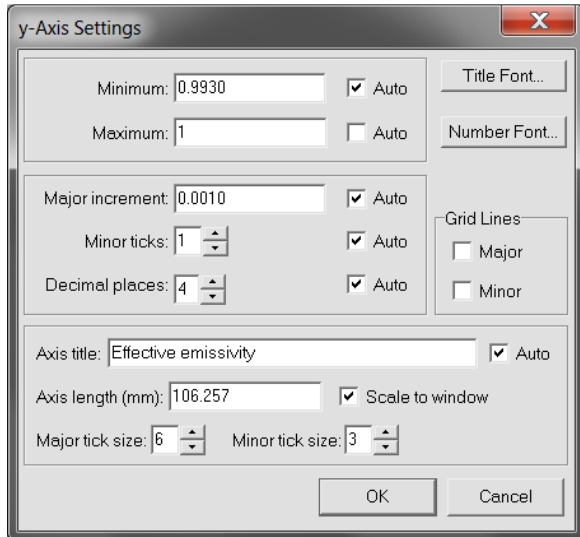


Figure 6. The dialog box used for scaling the graph axes.

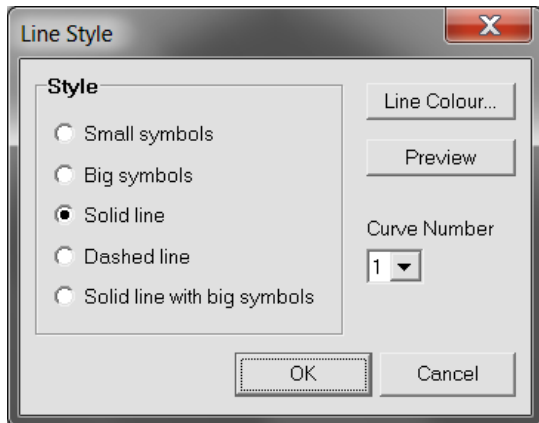


Figure 7. The dialog box used for setting the graph's line style.

#### Local Effective Emissivity Data

The data corresponding to the graph plotted in the `Emissivity Graph` panel is displayed in the `Emissivity Data` panel. This data can be copied and pasted into

other applications for further analysis. The data in each column can be formatted as either `General`, `Decimal`, or `Scientific` format through the `Edit|Format Column` menu (see Figure 8). The column with text selected is the one that is formatted, or if both columns have text selected, both columns will be formatted the same way. Individual column formats can be saved as default values, or the default values can be loaded, using the buttons on the lower left of the dialog box shown in Figure 8.

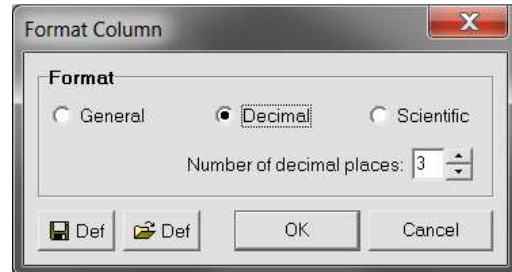


Figure 8. The dialog box used for setting the format of the columns in the `Emissivity Data` panel.

#### Calculating the Integrated Emissivity

The integrated emissivity is a weighted average of the local effective emissivities along the part of the cavity within the field of view of a radiation thermometer, and comprises umbral (fully detected) and penumbral (partially-vignetted) regions. The integrated emissivity is the cavity emissivity,  $\epsilon_{bb}$ , seen by the thermometer. In order to calculate  $\epsilon_{bb}$ , several parameters of the thermometer must be entered by selecting the `Cavity|Calculate Integrated Emissivity (Ebb)` menu or by clicking on the `Ebb` button on the tool bar. This brings up the dialog box shown in Figure 9.

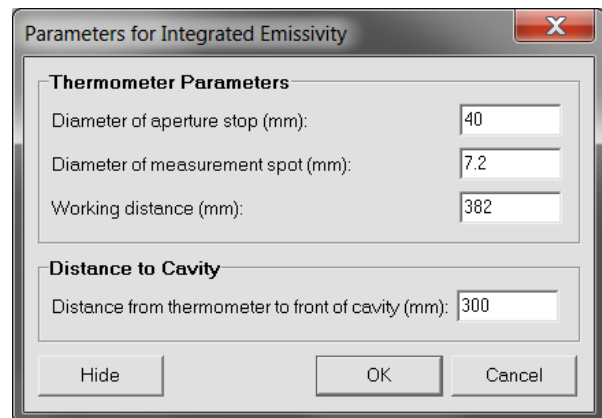


Figure 9. The dialog box used for entering the thermometer parameters for calculating the integrated emissivity.

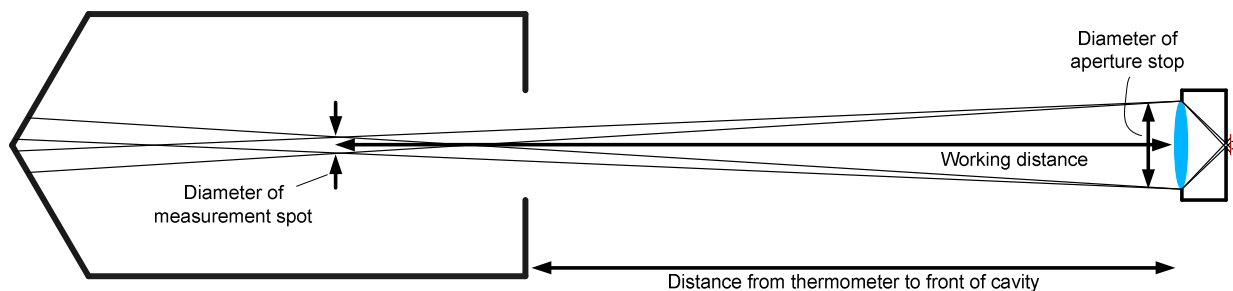


Figure 10. The four thermometer parameters required to calculate the integrated emissivity.

The required parameters are illustrated in Figure 10. The `Diameter of aperture stop` is the diameter of the thermometer's aperture stop inside its optical system. If this is unknown, then it may be approximated by the diameter of the thermometer's lens. The `Diameter of measurement spot` is the diameter of the field of view at the focal point of the optical system (the 'spot size'). The `Working distance` is the distance from the aperture stop to the focal point (approximately the distance from the front of the lens to the focal point). Finally, the `Distance from thermometer to front of cavity` is the measurement distance from the cavity.

Once valid values of all these parameters have been entered (and provided valid cavity parameters have also been entered), a sketch of the radiation thermometer with the limiting rays for the umbral and penumbral regions of the field of view is drawn in the `Cavity Schematic` panel. This gives a visual representation of the part of the cavity viewed by the thermometer. If the limiting rays do not all pass through the cavity aperture, then a `Warning Vignetting` message is displayed in the `Cavity Schematic` panel heading. In this case the integrated emissivity cannot be calculated. The cavity schematic can be copied to the clipboard or printed through the `Cavity` menu, or by right-clicking in the `Cavity Schematic` panel to bring up a pop-up menu.

When valid thermometer parameters have been entered, clicking on the `OK` button causes the integrated emissivity to be calculated. The result is given in the `Parameters` panel, along with all the parameters entered for the cavity and the thermometer. Data in the `Parameters` panel can be copied to the clipboard by right-clicking the mouse to bring up a pop-up menu. Note that `Ctrl+C` only copies data from the `Emissivity Data` spreadsheet.

### Examples of Thermometer Parameters

The thermometer parameters shown in the dialog box in Figure 9, and the schematic shown in Figure 10, correspond to a Heitronics TRT-II reference radiation thermometer. This thermometer is a fixed-focus device and has a minimum spot size (diameter) of 7.2 mm at a distance of 382 mm from the front of its lens. While the size of the aperture stop is not given in the specifications, it is reasonable to assume that it is roughly equal to the diameter of the lens, which is 40 mm. In the example given, the thermometer is focused part-way down the length of the cavity. Setting the measurement distance to 382 mm instead of 300 mm would focus the thermometer on the aperture of the cavity, resulting in a larger field of view on the conical part of the cavity, while setting the distance to 147.4 mm ( $= \text{working distance} - L_{\text{cav}} - L_{\text{cone}}$ ) would focus the thermometer on the apex of the cone, resulting in the smallest possible field of view on the cone.

A second example is shown in Figure 11, for a Raytek 8–14  $\mu\text{m}$  general-purpose radiation thermometer, with a specified distance-to-spot-size ratio (D:S) of 12:1. Further investigation of the specifications reveals that this D:S ratio strictly holds only at a measurement distance of 900 mm, where the spot size diameter is 75 mm. The diameter of the lens was measured to be 19.5 mm. Thus, Figure 11 results from setting the `Diameter of aperture stop` to 19.5 mm, the `Diameter of measurement spot` to 75 mm, and the `Working distance` to 700 mm.

For focusable systems, the working distance and spot size will change as the focus is adjusted, but the aperture stop diameter will remain the same. The specifications of such systems ideally should specify how the minimum spot size changes with focal distance, and the appropriate values can be entered into the software for a given focus setting.

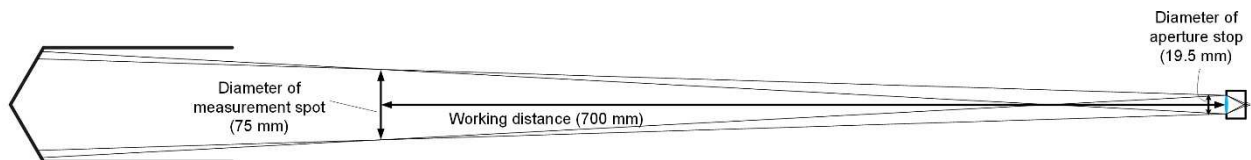


**Figure 11.** Field of view of a Raytek 8–14  $\mu\text{m}$  general-purpose radiation thermometer.

## Appendix A: Calculation of the Local Effective Emissivity

The local effective emissivity along each surface of the cavity is determined using the methods of Bedford and Ma [3, 4]. (Note that there are a few typographical errors in the equations in the original Bedford and Ma papers, which are corrected here.) For cavities with a cone, distances along the cone axis are denoted by the coordinate  $x$ , such that  $0 \leq x \leq L_{\text{cone}}$  (refer to Figure 4), otherwise distances along the base of the cylinder, measured from the centre, are denoted by the coordinate  $r$ , where  $0 \leq r \leq R_{\text{cav}}$  and  $R_{\text{cav}} = D_{\text{cav}}/2$ . Distances along the length of the cylinder wall are denoted by the coordinate  $y$ , where  $L_{\text{cone}} \leq y \leq L_{\text{cone}} + L_{\text{cav}}$ , and, finally, distances along the inside of the aperture lid (when one exists) are denoted by the coordinate  $z$ , such that  $R_{\text{aper}} \leq z \leq R_{\text{cav}}$ , where  $R_{\text{aper}} = D_{\text{aper}}/2$ .

At each point, the local effective emissivity is equal to the ratio of the radiant flux leaving that point, including reflected flux from other surfaces, to the flux that would leave it if it were black. Because of the axial symmetry, the calculations can be performed for infinitesimal bands around each surface rather than individual points. For example, the local effective emissivity of an infinitesimal band of width  $dy$  and area  $dA_{y_0}$  on the cylinder wall, centred on the coordinate  $y_0$  where the temperature is  $T_{y_0}$ , is given by

$$\varepsilon_{\text{eff}}(y_0, \lambda, T_{y_0}, T_0) = \frac{L(y_0, \lambda, T_{y_0})}{L_b(\lambda, T_0)}, \quad (\text{A1})$$

where  $L(y_0, \lambda, T_{y_0})$  is the spectral radiance of  $dA_{y_0}$ ,  $L_b(\lambda, T_0)$  is the spectral radiance of a blackbody at temperature  $T_0$ , and  $\lambda$  is the wavelength. For all calculations,  $T_0$  is taken to be the temperature at the apex of the cone or the centre of the base of the cavity, as appropriate.

Equations similar to equation (A1) can be written for infinitesimal bands on the other surfaces within the cavity, so that equation (A1) can be written in terms of these other local effective emissivities, and in terms of just blackbody radiances:

$$\begin{aligned} \varepsilon_{\text{eff}}(y_0, \lambda, T_{y_0}, T_0) &= \varepsilon(y_0, \lambda, T_{y_0}) \frac{L_b(\lambda, T_{y_0})}{L_b(\lambda, T_0)} \\ &+ [1 - \varepsilon(y_0, \lambda, T_{y_0})] \int_0^{L_{\text{cone}}} \varepsilon_{\text{eff}}(x, \lambda, T_x, T_0) d^2F_{y_0, x} \\ &+ [1 - \varepsilon(y_0, \lambda, T_{y_0})] \int_{L_{\text{cone}}}^{L_{\text{cone}} + L_{\text{cav}}} \varepsilon_{\text{eff}}(y, \lambda, T_y, T_0) d^2F_{y_0, y} \\ &+ [1 - \varepsilon(y_0, \lambda, T_{y_0})] \int_{R_{\text{aper}}}^{R_{\text{cav}}} \varepsilon_{\text{eff}}(z, \lambda, T_z, T_0) d^2F_{y_0, z} \\ &+ [1 - \varepsilon(y_0, \lambda, T_{y_0})] \int_0^{R_{\text{cav}}} \varepsilon_{\text{eff}}(r, \lambda, T_r, T_0) d^2F_{y_0, r} \end{aligned} \quad (\text{A2})$$

where  $\varepsilon(y_0, \lambda, T_{y_0})$  is the intrinsic emissivity of the surface of the cylinder wall at position  $y_0$ , wavelength  $\lambda$ , and temperature  $T_{y_0}$ . The software assumes this to be constant for all positions along the cylinder wall, for all wavelengths, and for all temperatures, so that  $\varepsilon(y_0, \lambda, T_{y_0}) = \varepsilon_{\text{cav}}$ . The quantity  $d^2F_{y_0, x}$  is the angle factor for radiant exchange between  $dA_{y_0}$  on the cylinder and  $dA_x$  on the cone [8]. Similar definitions hold for the other  $d^2F$  quan-

ties. Terms on the right-hand side of equation (A2) corresponding to non-existent surfaces (depending on the chosen geometry) are left out of the equation.

Similar equations hold for the local effective emissivities of infinitesimal bands on the other surfaces, resulting in a set of simultaneous integral equations to be solved for the entire interior surface of the cavity. The method of solution is to divide each of the integrals into a number,  $n$ , of equal parts, where, for large enough  $n$ , it can be reasonably assumed that the local effective emissivity within each interval is constant. Each integral then becomes a sum of  $n$  sub-integrals that can be evaluated analytically by suitable single differentiation of the angle factor between two parallel circular disks with a common central normal. Thus, the  $d^2F$  quantities can be replaced with  $dF$  quantities (angle factors between an infinitesimal area and a finite disk) [8]. Finally, to take account of the finite bandwidth of the radiation thermometer viewing the cavity, the ratio of spectral radiances in equation (A2) is replaced by the ratio of thermometer signals given by the Sakuma–Hattori equation (equation (7)):

$$\frac{L_b(\lambda, T_{y_0})}{L_b(\lambda, T_0)} \Rightarrow \frac{S(T_{y_0})}{S(T_0)}. \quad (\text{A3})$$

If the cavity is isothermal, then this ratio is unity and the local effective emissivity is independent of wavelength.

### Solution for Cavities with a Flat Base

When the cavity has the form shown in Figure 4(a), the simplifications discussed above result in three simultaneous analytical equations to be solved. Note that the cylinder wall can see other parts of the cylinder wall as well as the base and the lid. However, the base and the lid cannot see other parts of themselves. Thus, the three equations are:

$$\begin{aligned} \varepsilon_{\text{eff}}(y_0) &= \varepsilon_{\text{cav}} \frac{S(T_{y_0})}{S(T_0)} \\ &+ (1 - \varepsilon_{\text{cav}}) \sum_{j=1}^n 0.5 [\varepsilon_{\text{eff}}(y_{j+1}) + \varepsilon_{\text{eff}}(y_j)] [dF_{y_0, y_{j+1}} - dF_{y_0, y_j}] \\ &+ (1 - \varepsilon_{\text{cav}}) \sum_{k=1}^n 0.5 [\varepsilon_{\text{eff}}(z_{k+1}) + \varepsilon_{\text{eff}}(z_k)] [dF_{y_0, z_{k+1}} - dF_{y_0, z_k}] \\ &+ (1 - \varepsilon_{\text{cav}}) \sum_{p=1}^n 0.5 [\varepsilon_{\text{eff}}(r_{p+1}) + \varepsilon_{\text{eff}}(r_p)] [dF_{y_0, r_{p+1}} - dF_{y_0, r_p}] \end{aligned} \quad (\text{A4})$$

$$\begin{aligned} \varepsilon_{\text{eff}}(z_0) &= \varepsilon_{\text{aper}} \frac{S(T_{z_0})}{S(T_0)} \\ &+ (1 - \varepsilon_{\text{aper}}) \sum_{j=1}^n 0.5 [\varepsilon_{\text{eff}}(y_{j+1}) + \varepsilon_{\text{eff}}(y_j)] [dF_{z_0, y_{j+1}} - dF_{z_0, y_j}] \\ &+ (1 - \varepsilon_{\text{aper}}) \sum_{p=1}^n 0.5 [\varepsilon_{\text{eff}}(r_{p+1}) + \varepsilon_{\text{eff}}(r_p)] [dF_{z_0, r_{p+1}} - dF_{z_0, r_p}] \end{aligned} \quad (\text{A5})$$

$$\begin{aligned} \varepsilon_{\text{eff}}(r_0) &= \varepsilon_{\text{base}} \frac{S(T_{r_0})}{S(T_0)} \\ &+ (1 - \varepsilon_{\text{base}}) \sum_{j=1}^n 0.5 [\varepsilon_{\text{eff}}(y_{j+1}) + \varepsilon_{\text{eff}}(y_j)] [dF_{r_0, y_{j+1}} - dF_{r_0, y_j}] \\ &+ (1 - \varepsilon_{\text{base}}) \sum_{k=1}^n 0.5 [\varepsilon_{\text{eff}}(z_{k+1}) + \varepsilon_{\text{eff}}(z_k)] [dF_{r_0, z_{k+1}} - dF_{r_0, z_k}] \end{aligned} \quad (\text{A6})$$

where the local effective emissivity within each interval is taken to be the mean of the values calculated at the boundaries of the interval, and  $y_1 = 0$ ,  $y_{n+1} = L_{\text{cav}}$ ,  $z_1 = R_{\text{aper}}$ ,  $z_{n+1} = R_{\text{cav}}$ ,  $r_1 = 0$ , and  $r_{n+1} = R_{\text{cav}}$ . The equations are solved iteratively by initially setting each of the

$\varepsilon_{\text{eff}}$  values to the intrinsic emissivity of the corresponding surface and calculating new  $\varepsilon_{\text{eff}}$  values, then repeating these calculations until the maximum change of all the individual  $\varepsilon_{\text{eff}}$  values is smaller than a predetermined tolerance. The  $dF$  angle factors are calculated as follows:

$$dF_{y_0, y_j} = \frac{[(y_j - y_0)^2 + 4R_{\text{cav}}^2]^{1/2}}{2R_{\text{cav}}} - \frac{R_{\text{cav}}}{[(y_j - y_0)^2 + 4R_{\text{cav}}^2]^{1/2}} - \frac{|y_j - y_0|}{2R_{\text{cav}}} \quad (\text{A7})$$

$$dF_{y_0, r_p} = \frac{y_0}{2R_{\text{cav}}} \left\{ \frac{y_0^2 + r_p^2 + R_{\text{cav}}^2}{[(y_0^2 + r_p^2 + R_{\text{cav}}^2)^2 - 4r_p^2 R_{\text{cav}}^2]^{1/2}} - 1 \right\} \quad (\text{A8})$$

$$dF_{y_0, z_k} = \frac{L_{\text{cav}} - y_0}{2R_{\text{cav}}} \left\{ \frac{(L_{\text{cav}} - y_0)^2 + z_k^2 + R_{\text{cav}}^2}{\left[ \left[ (L_{\text{cav}} - y_0)^2 + z_k^2 + R_{\text{cav}}^2 \right]^2 - 4z_k^2 R_{\text{cav}}^2 \right]^{1/2}} - 1 \right\} \quad (\text{A9})$$

$$dF_{r_0, y_j} = \frac{1}{2} \left\{ 1 - \frac{y_j^2 + r_0^2 - R_{\text{cav}}^2}{[(y_j^2 + r_0^2 + R_{\text{cav}}^2)^2 - 4r_0^2 R_{\text{cav}}^2]^{1/2}} \right\} \quad (\text{A10})$$

$$dF_{r_0, z_k} = \frac{1}{2} \left\{ 1 - \frac{L_{\text{cav}}^2 + r_0^2 - z_k^2}{\left[ (L_{\text{cav}}^2 + r_0^2 + z_k^2)^2 - 4r_0^2 z_k^2 \right]^{1/2}} \right\} \quad (\text{A11})$$

$$dF_{z_0, y_j} = \frac{1}{2} \left\{ 1 - \frac{(L_{\text{cav}} - y_j)^2 + z_0^2 - R_{\text{cav}}^2}{\left[ \left[ (L_{\text{cav}} - y_j)^2 + z_0^2 + R_{\text{cav}}^2 \right]^2 - 4z_0^2 R_{\text{cav}}^2 \right]^{1/2}} \right\} \quad (\text{A12})$$

$$dF_{z_0, r_p} = \frac{1}{2} \left\{ 1 - \frac{L_{\text{cav}}^2 + z_0^2 - r_p^2}{\left[ (L_{\text{cav}}^2 + z_0^2 + r_p^2)^2 - 4z_0^2 r_p^2 \right]^{1/2}} \right\} \quad (\text{A13})$$

Singularities occur in the above equations at locations corresponding to the intersection of the cylinder wall with either the base or the aperture plate. That is, when  $y_0 = 0$  and  $r_p = R_{\text{cav}}$ , when  $y_0 = L_{\text{cav}}$  and  $z_k = R_{\text{cav}}$ , when  $y_j = 0$  and  $r_0 = R_{\text{cav}}$ , and when  $y_j = L_{\text{cav}}$  and  $z_0 = R_{\text{cav}}$ . In all of these cases, it can be shown using L'Hôpital's rule that the limiting value for each of the appropriate  $dF$  quantities is equal to 0.5. These singularities are avoided by replacing the last term in the second sum of equation (A4) by  $0.5\varepsilon_{\text{eff}}(z_{n+1})$  when  $y_0 = 0$ , and the last term in the third sum of equation (A4) by  $0.5\varepsilon_{\text{eff}}(r_{n+1})$  when  $y_0 = L_{\text{cav}}$ . Additionally, when  $z_0 = R_{\text{cav}}$ , the last in term in the first sum of equation (A5) should be replaced by

$$0.5\varepsilon_{\text{eff}}(y_{n+1}) + 0.5[\varepsilon_{\text{eff}}(y_{n+1}) + \varepsilon_{\text{eff}}(y_n)][0.5 - F_{R_{\text{cav}}, y_n}],$$

and when  $r_0 = R_{\text{cav}}$ , the first term in the first sum of equation (A6) should be replaced by

$$0.5\varepsilon_{\text{eff}}(y_1) + 0.5[\varepsilon_{\text{eff}}(y_1) + \varepsilon_{\text{eff}}(y_2)][0.5 - F_{R_{\text{cav}}, y_2}].$$

#### Solution for Cavities with a Conical Base

When the cavity has the form of either Figure 4(b) or 4(c), the equations to be solved for the local effective emissivity of the cone wall, the cylinder wall, and the aperture plate are:

$$\begin{aligned} \varepsilon_{\text{eff}}(x_0) = & \varepsilon_{\text{cone}} \frac{S(T_{x_0})}{S(T_0)} \quad (\text{A14}) \\ & + (1 - \varepsilon_{\text{cone}}) \sum_{i=1}^n 0.5 [\varepsilon_{\text{eff}}(x_{i+1}) + \varepsilon_{\text{eff}}(x_i)] [dF_{x_0, x_{i+1}} - dF_{x_0, x_i}] \\ & + (1 - \varepsilon_{\text{cone}}) \sum_{j=1}^n 0.5 [\varepsilon_{\text{eff}}(y_{j+1}) + \varepsilon_{\text{eff}}(y_j)] [dF_{x_0, y_{j+1}} - dF_{x_0, y_j}] \\ & + (1 - \varepsilon_{\text{cone}}) \sum_{k=1}^n 0.5 [\varepsilon_{\text{eff}}(z_{k+1}) + \varepsilon_{\text{eff}}(z_k)] [dF_{x_0, z_{k+1}} - dF_{x_0, z_k}] \end{aligned}$$

$$\begin{aligned} \varepsilon_{\text{eff}}(y_0) &= \varepsilon_{\text{cav}} \frac{S(T_{y_0})}{S(T_0)} \\ &+ (1 - \varepsilon_{\text{cav}}) \sum_{i=1}^n 0.5 [\varepsilon_{\text{eff}}(x_{i+1}) + \varepsilon_{\text{eff}}(x_i)] [dF_{y_0, x_{i+1}} - dF_{y_0, x_i}] \\ &+ (1 - \varepsilon_{\text{cav}}) \sum_{j=1}^n 0.5 [\varepsilon_{\text{eff}}(y_{j+1}) + \varepsilon_{\text{eff}}(y_j)] [dF_{y_0, y_{j+1}} - dF_{y_0, y_j}] \\ &+ (1 - \varepsilon_{\text{cav}}) \sum_{k=1}^n 0.5 [\varepsilon_{\text{eff}}(z_{k+1}) + \varepsilon_{\text{eff}}(z_k)] [dF_{y_0, z_{k+1}} - dF_{y_0, z_k}] \end{aligned} \quad (\text{A15})$$

$$\begin{aligned} \varepsilon_{\text{eff}}(z_0) &= \varepsilon_{\text{aper}} \frac{S(T_{z_0})}{S(T_0)} \\ &+ (1 - \varepsilon_{\text{aper}}) \sum_{i=1}^n 0.5 [\varepsilon_{\text{eff}}(x_{i+1}) + \varepsilon_{\text{eff}}(x_i)] [dF_{z_0, x_{i+1}} - dF_{z_0, x_i}] \\ &+ (1 - \varepsilon_{\text{aper}}) \sum_{j=1}^n 0.5 [\varepsilon_{\text{eff}}(y_{j+1}) + \varepsilon_{\text{eff}}(y_j)] [dF_{z_0, y_{j+1}} - dF_{z_0, y_j}] \end{aligned} \quad (\text{A16})$$

where  $x_1 = 0$ ,  $x_{n+1} = L_{\text{cone}}$ ,  $y_1 = L_{\text{cone}}$ ,  $y_{n+1} = L_{\text{cone}} + L_{\text{cav}}$ ,  $z_1 = R_{\text{aper}}$ , and  $z_{n+1} = R_{\text{cav}}$ . The  $dF$  angle factors are calculated as follows, where the angle  $\alpha$  is the half-angle of the cone; i.e.,  $\alpha = \theta/2$ :

$$dF_{x_0, x_i} = f_i \pm \left[ \frac{x_i \cos^2 \alpha}{2x_0 \sin \alpha} - \frac{1}{2 \sin \alpha} \right] \begin{cases} + & \text{for } x_i < x_0 \\ - & \text{for } x_i \geq x_0 \end{cases} \quad (\text{A17})$$

where

$$f_i = \frac{[(x_i + x_0)^2 - 4x_i x_0 \cos^2 \alpha]^{1/2}}{4x_0 \sin \alpha} \left[ 1 + \frac{(x_0 - x_i)(x_i + x_0 - 2x_i \cos^2 \alpha)}{(x_i + x_0)^2 - 4x_i x_0 \cos^2 \alpha} \right] \quad (\text{A18})$$

$$dF_{x_0, y_j} = \frac{\sin \alpha}{2} - \frac{\cos^2 \alpha}{2x_0 \sin \alpha} \left\{ y_j - x_0 + \frac{[R_{\text{cav}}^2 + x_0^2 \tan^2 \alpha + (y_j - x_0)^2][x_0 \tan^2 \alpha - (y_j - x_0)] - 2R_{\text{cav}}^2 x_0 \tan^2 \alpha}{\left\{ [R_{\text{cav}}^2 + x_0^2 \tan^2 \alpha + (y_j - x_0)^2]^2 - 4R_{\text{cav}}^2 x_0^2 \tan^2 \alpha \right\}^{1/2}} \right\} \quad (\text{A19})$$

$$dF_{x_0, z_k} = \frac{\sin \alpha}{2} - \frac{\cos^2 \alpha}{2x_0 \sin \alpha} \left\{ L_{\text{cone}} + L_{\text{cav}} - x_0 + \frac{[z_k^2 + x_0^2 \tan^2 \alpha + (L_{\text{cone}} + L_{\text{cav}} - x_0)^2][x_0 \tan^2 \alpha - (L_{\text{cone}} + L_{\text{cav}} - x_0)] - 2z_k^2 x_0 \tan^2 \alpha}{\left\{ [z_k^2 + x_0^2 \tan^2 \alpha + (L_{\text{cone}} + L_{\text{cav}} - x_0)^2]^2 - 4z_k^2 x_0^2 \tan^2 \alpha \right\}^{1/2}} \right\} \quad (\text{A20})$$

$$dF_{y_0, x_i} = \frac{y_0 - x_i}{2R_{\text{cav}}} \left\{ \frac{R_{\text{cav}}^2 + x_i^2 \tan^2 \alpha + (y_0 - x_i)^2}{\left\{ [R_{\text{cav}}^2 + x_i^2 \tan^2 \alpha + (y_0 - x_i)^2]^2 - 4x_i^2 R_{\text{cav}}^2 \tan^2 \alpha \right\}^{1/2}} - 1 \right\} \quad (\text{A21})$$

$$dF_{y_0, y_j} = \frac{[(y_j - y_0)^2 + 4R_{\text{cav}}^2]^{1/2}}{2R_{\text{cav}}} - \frac{R_{\text{cav}}}{[(y_j - y_0)^2 + 4R_{\text{cav}}^2]^{1/2}} - \frac{|y_j - y_0|}{2R_{\text{cav}}} \quad (\text{A22})$$

$$dF_{y_0, z_k} = \frac{L_{\text{cone}} + L_{\text{cav}} - y_0}{2R_{\text{cav}}} \left\{ \frac{(L_{\text{cone}} + L_{\text{cav}} - y_0)^2 + z_k^2 + R_{\text{cav}}^2}{\left\{ [(L_{\text{cone}} + L_{\text{cav}} - y_0)^2 + z_k^2 + R_{\text{cav}}^2]^2 - 4z_k^2 R_{\text{cav}}^2 \right\}^{1/2}} - 1 \right\} \quad (\text{A23})$$

$$dF_{z_0, x_i} = \frac{1}{2} \left\{ 1 - \frac{z_0^2 + (L_{\text{cone}} + L_{\text{cav}} - x_i)^2 - x_i^2 \tan^2 \alpha}{\left\{ [z_0^2 + (L_{\text{cone}} + L_{\text{cav}} - x_i)^2 + x_i^2 \tan^2 \alpha]^2 - 4z_0^2 x_i^2 \tan^2 \alpha \right\}^{1/2}} \right\} \quad (\text{A24})$$

$$dF_{z_0, y_j} = \frac{1}{2} \left\{ 1 - \frac{z_0^2 + (L_{\text{cone}} + L_{\text{cav}} - y_j)^2 - R_{\text{cav}}^2}{\left\{ [z_0^2 + (L_{\text{cone}} + L_{\text{cav}} - y_j)^2 + R_{\text{cav}}^2]^2 - 4z_0^2 R_{\text{cav}}^2 \right\}^{1/2}} \right\} \quad (\text{A25})$$

A singular occurs in equations (A17) to (A20) when  $x_0 = 0$ ; that is, at the apex of the cone. Using L'Hôpital's

rule, the correct expression for the local effective emissivity at the apex can be shown to be

$$\begin{aligned} \varepsilon_{\text{eff}}(x_0 = 0) = & \left\{ \varepsilon_{\text{cone}} + (1 - \varepsilon_{\text{cone}}) \sin \alpha \sum_{j=1}^n 0.5 [\varepsilon_{\text{eff}}(y_{j+1}) + \varepsilon_{\text{eff}}(y_j)] \left[ \frac{R_{\text{cav}}^2}{R_{\text{cav}}^2 + y_j^2} - \frac{R_{\text{cav}}^2}{R_{\text{cav}}^2 + y_{j+1}^2} \right] \right. \\ & \left. + (1 - \varepsilon_{\text{cone}}) \sin \alpha \sum_{k=1}^n 0.5 [\varepsilon_{\text{eff}}(z_{k+1}) + \varepsilon_{\text{eff}}(z_k)] \left[ \frac{z_{k+1}^2}{z_{k+1}^2 + (L_{\text{cone}} + L_{\text{cav}})^2} - \frac{z_k^2}{z_k^2 + (L_{\text{cone}} + L_{\text{cav}})^2} \right] \right\} / \left[ \varepsilon_{\text{cone}} + (1 - \varepsilon_{\text{cone}}) \sin^3 \alpha \right]. \end{aligned} \quad (\text{A26})$$

Other singularities occur at the intersection of the conical section of the cavity with the cylindrical section (or the aperture lid, if there is no cylindrical section), and at the intersection of the cylindrical section and the aperture lid. These singularities are resolved as follows.

When there is no cylindrical section, and when  $x_0 = L_{\text{cone}}$ , the last term in the third sum of equation (A14) should be replaced by

$$0.5 \varepsilon_{\text{eff}}(z_{n+1})(1 + \sin \alpha).$$

When  $z_0 = R_{\text{cav}}$ , the last term in the first sum of equation (A16) should be replaced by

$$\begin{aligned} & 0.5 \varepsilon_{\text{eff}}(x_{n+1})(1 + \sin \alpha) \\ & + 0.5 [\varepsilon_{\text{eff}}(x_{n+1}) + \varepsilon_{\text{eff}}(x_n)] \left[ \frac{1 - \sin \alpha}{2} - dF_{R_{\text{cav}}, x_n} \right]. \end{aligned}$$

When there is a cylindrical section, and  $x_0 = L_{\text{cone}}$ , the first term in the second sum of equation (A14) should be replaced by

$$\begin{aligned} & 0.5 \varepsilon_{\text{eff}}(y_1)(1 - \cos \alpha) \\ & + 0.5 [\varepsilon_{\text{eff}}(y_1) + \varepsilon_{\text{eff}}(y_2)] \left[ \frac{\sin \alpha + \cos \alpha}{2} - dF_{L_{\text{cone}}, y_2} \right]. \end{aligned}$$

When  $y_0 = L_{\text{cone}}$  the last term in the first sum of equation (A15) should be replaced by

$$\begin{aligned} & 0.5 \varepsilon_{\text{eff}}(x_{n+1})(1 - \cos \alpha) \\ & + 0.5 [\varepsilon_{\text{eff}}(x_n) + \varepsilon_{\text{eff}}(x_{n+1})] \left[ \frac{\cos \alpha}{2} - dF_{L_{\text{cone}}, x_n} \right]. \end{aligned}$$

When  $y_0 = L_{\text{cone}} + L_{\text{cav}}$ , the last term in the third sum of equation (A15) should be replaced by  $0.5 \varepsilon_{\text{eff}}(z_{n+1})$ , and when  $z_0 = R_{\text{cav}}$ , the last term in the second sum of equation (A16) should be replaced by

$$0.5 \varepsilon_{\text{eff}}(y_{n+1}) + 0.5 [\varepsilon_{\text{eff}}(y_{n+1}) + \varepsilon_{\text{eff}}(y_n)] \left[ 0.5 - dF_{R_{\text{cav}}, y_n} \right].$$



$L_{\text{meas}}$  is the measurement distance (i.e., the distance from the front of the cavity to the apparent aperture stop), and  $R_{\text{stop}}$  is the radius of the apparent aperture stop. The value of  $x_1$ , the limit of the umbral region, can be determined by tracing the rays shown in Figure 1. The upper limit on the  $\rho$  integral is  $\rho_2 = 2R_{\text{stop}} \cos \varphi$ .

$$I_{x_1-x_2} = 4 \int_{x_1}^{x_2} \int_0^{\varphi_2} \int_0^{\rho_2} \varepsilon_{\text{eff}}(x) \cos \psi_x (L_{\text{cone}} + L_{\text{cav}} + L_{\text{meas}} - x) \frac{x \tan \alpha}{d^3 \cos \alpha} \rho d \rho d \varphi dx. \quad (\text{B5})$$

The equations for  $\cos \psi_x$  and  $d$  are again given by equations (B3) and (B4), respectively. The values of  $x_1$  and  $x_2$ , the limits of the umbral and penumbral regions, can be found by tracing the rays shown in Figure 1. The upper limit of the  $\varphi$  integral is given by

$$\varphi_2 = \cos^{-1} \sqrt{\frac{(R_{\text{stop}} + C_0)^2 - R_0^2}{4R_{\text{stop}}C_0}}, \quad (\text{B6})$$

where

$$C_0 = \left| \frac{xR_{\text{cav}}(x_{\text{spot}} - x_{\text{stop}})}{L_{\text{cone}}(x_{\text{spot}} - x)} \right| \quad (\text{B7})$$

and

$$R_0 = \left| \frac{R_{\text{spot}}(x_{\text{spot}} - x)}{(x_{\text{spot}} - x)} \right|. \quad (\text{B8})$$

Here  $x_{\text{spot}}$  is the  $x$ -coordinate, measured from the apex of the cone, of the location of the measurement spot (focal point),  $x_{\text{stop}}$  is the  $x$ -coordinate of the location of the apparent aperture stop (equal to  $L_{\text{cone}} + L_{\text{cav}} + L_{\text{meas}}$ ), and

#### Penumbra Region on the Cone

For the penumbral region, not all of the flux passing through the measurement spot intersects the apparent aperture stop. Thus, the contribution to the integral in the numerator of equation (B1) is similar to equation (B2), but with different limits on the  $x$ ,  $\varphi$  and  $\rho$  integrals:

$R_{\text{spot}}$  is the radius of the measurement spot at the focal point.

The limits of the  $\rho$  integral are

$$\rho_1 = (R_{\text{stop}} + C_0) \cos \varphi - [R_0^2 - (R_{\text{stop}} + C_0)^2 \sin^2 \varphi]^{1/2} \quad (\text{B9})$$

and

$$\rho_2 = 2R_{\text{stop}} \cos \varphi. \quad (\text{B10})$$

If the umbral and penumbral regions fall entirely on the cone, then the integrated emissivity is given by

$$\varepsilon_{\text{bb}} = \frac{I_{0-x_1} + I_{x_1-x_2}}{I_{0-x_1}^b + I_{x_1-x_2}^b}, \quad (\text{B11})$$

where  $I_{0-x_1}^b$  and  $I_{x_1-x_2}^b$  are given by equations (B2) and (B5), respectively, but with  $\varepsilon_{\text{eff}}(x) = 1$  for all values of  $x$ . When the umbral or penumbral regions are not entirely on the cone, additional sums to the integrals need to be included from parts of the cylinder wall (see below).

#### Umbral Region on the Flat Base

The contribution to the integral in the numerator of equation (B1) from the flux intersecting the apparent aperture stop from the umbral region on the flat base is:

$$I_{0-r_1} = 4(L_{\text{cav}} + L_{\text{meas}})^2 \int_0^{r_1} \int_0^{\pi/2} \int_0^{\rho_2} \varepsilon_{\text{eff}}(r) \frac{r}{d^4} \rho d \rho d \varphi dr, \quad (\text{B12})$$

where

$$d = [(\rho \cos \varphi + r - R_{\text{stop}})^2 + (\rho \sin \varphi)^2 + (L_{\text{cav}} + L_{\text{meas}})^2]^{1/2}, \quad (\text{B13})$$

and the upper limit on the  $\rho$  integral is again  $\rho_2 = 2R_{\text{stop}} \cos \varphi$ . The value of  $r_1$ , the limit of the umbral region, can be determined by tracing the rays shown in Figure 1.

#### Penumbra Region on the Flat Base

For the penumbral region, the contribution to the integral in the numerator of equation (B1) is similar to equation (B12), but with different limits on the  $r$ ,  $\varphi$  and  $\rho$  integrals:

$$I_{r_1-r_2} = 4(L_{\text{cav}} + L_{\text{meas}})^2 \int_{r_1}^{r_2} \int_0^{\varphi_2} \int_0^{\rho_2} \varepsilon_{\text{eff}}(r) \frac{r}{d^4} \rho d \rho d \varphi dr. \quad (\text{B14})$$

The equation for  $d$  is again given by equation (B13). The values of  $r_1$  and  $r_2$ , the limits of the umbral and penumbral regions, can be found by tracing the rays shown in Figure 1. The upper limit of the  $\varphi$  integral is given by equation (B6), but in this case

$$C_0 = \left| \frac{r(x_{\text{spot}} - x_{\text{stop}})}{x_{\text{spot}}} \right| \quad (\text{B15})$$

and

$$R_0 = \left| \frac{R_{\text{spot}} x_{\text{stop}}}{x_{\text{spot}}} \right|. \quad (\text{B16})$$

The coordinates  $x_{\text{spot}}$  and  $x_{\text{stop}}$  are this time measured from the base of the cavity.

If the umbral and penumbral regions fall entirely on the flat base, then the integrated emissivity is given by

$$\varepsilon_{\text{bb}} = \frac{I_{0-r_1} + I_{r_1-r_2}}{I_{0-r_1}^{\text{p}} + I_{r_1-r_2}^{\text{p}}}, \quad (\text{B17})$$

$$I_{L_{\text{cone}}-y_1} = 4R_{\text{cav}} \int_{L_{\text{cone}}}^{y_1} \int_0^{\pi/2} \int_0^{\rho_2} \varepsilon_{\text{eff}}(y) \cos \psi_y \frac{(L_{\text{cone}} + L_{\text{cav}} + L_{\text{meas}} - y)}{d^3} \rho d\rho d\varphi dy, \quad (\text{B18})$$

where

$$\cos \psi_y = \frac{R_{\text{cav}} - R_{\text{stop}} + \rho \cos \varphi}{d}, \quad (\text{B19})$$

$$d = \left[ (\rho \cos \varphi + R_{\text{cav}} - R_{\text{stop}})^2 + (\rho \sin \varphi)^2 + (L_{\text{cone}} + L_{\text{cav}} + L_{\text{meas}} - y)^2 \right]^{1/2}, \quad (\text{B20})$$

and the upper limit on the  $\rho$  integral is again  $\rho_2 = 2R_{\text{stop}} \cos \varphi$ . The value of  $y_1$ , the limit of the umbral region, can be determined by tracing the rays shown in Figure 1.

where  $I_{0-r_1}^{\text{p}}$  and  $I_{r_1-r_2}^{\text{p}}$  are given by equations (B12) and (B14), respectively, but with  $\varepsilon_{\text{eff}}(r) = 1$  for all values of  $r$ . When the umbral or penumbral regions are not entirely on the flat base, additional sums to the integrals need to be included from parts of the cylinder wall (see below).

#### Umbral Region on the Cylinder Wall

The contribution to the integral in the numerator of equation (B1) from the flux intersecting the apparent aperture stop from the umbral region on the cylinder wall is:

#### Penumbral Region on the Cylinder Wall

For the penumbral region, the contribution to the integral in the numerator of equation (B1) is similar to equation (B18), but with different limits on the  $y$ ,  $\varphi$  and  $\rho$  integrals:

$$I_{y_1-y_2} = 4R_{\text{cav}} \int_{y_1}^{y_2} \int_0^{\varphi_2} \int_{\rho_1}^{\rho_2} \varepsilon_{\text{eff}}(y) \cos \psi_y \frac{(L_{\text{cone}} + L_{\text{cav}} + L_{\text{meas}} - y)}{d^3} \rho d\rho d\varphi dy. \quad (\text{B21})$$

The equations for  $\cos \psi_y$  and  $d$  are given by equations (B19) and (B20), respectively. The values of  $y_1$  and  $y_2$ , the limits of the umbral and penumbral regions, can be found by tracing the rays shown in Figure 1. The upper limit of the  $\varphi$  integral is given by equation (B6), but in this case

$$C_0 = \left| \frac{R_{\text{cav}} (x_{\text{spot}} - x_{\text{stop}})}{(x_{\text{spot}} - y)} \right| \quad (\text{B22})$$

and

$$R_0 = \left| \frac{R_{\text{spot}} (x_{\text{stop}} - y)}{(x_{\text{spot}} - y)} \right|. \quad (\text{B23})$$

The coordinates  $x_{\text{spot}}$  and  $x_{\text{stop}}$  are this time measured from the apex of the cone (if there is a cone) or otherwise from the centre of the flat base of the cavity.

The integrated emissivity will necessarily include contributions from either the cone or the flat base. For example, if there is a cone and the umbral region spills over to the cylinder wall, then the integrated emissivity is equal to

$$\varepsilon_{\text{bb}} = \frac{I_{0-L_{\text{cone}}} + I_{L_{\text{cone}}-y_1} + I_{y_1-y_2}}{I_{0-L_{\text{cone}}}^{\text{p}} + I_{L_{\text{cone}}-y_1}^{\text{p}} + I_{y_1-y_2}^{\text{p}}}, \quad (\text{B24})$$

where  $I_{L_{\text{cone}}-y_1}^{\text{p}}$  and  $I_{y_1-y_2}^{\text{p}}$  are given by equations (B18) and (B21), respectively, but with  $\varepsilon_{\text{eff}}(y) = 1$  for all values of  $y$ .

#### Gauss–Legendre Integration

Each of the three-dimensional integrals given by equations (B2), (B5), (B12), (B14), B(18), and B(21), and their corresponding black versions, must be evaluated numerically, which can be very time consuming if the integrals are divided into a large number,  $N$ , of steps (each integral requires  $N^3$  integrand evaluations). In order to reduce the calculation time, the software employs Gauss–Legendre integration [10], which is based on the method of Gaussian quadratures.

In one dimension, Gauss–Legendre integration is implemented as

$$\int_a^b f(x) dx = \frac{b-a}{2} \sum_{i=1}^N w_i f\left(\frac{b-a}{2} x_i + \frac{a+b}{2}\right), \quad (\text{B25})$$

where the  $x_i$  values are fixed numbers between  $-1$  and  $+1$ , and the  $w_i$  values are corresponding fixed weights. Remarkably, equation (B25), which consists of  $N$  function evaluations, is exact when  $f(x)$  is a polynomial with order up to  $2N-1$ . Note that the  $x_i$  and  $w_i$  values apply to any  $f(x)$  that can be approximated by a polynomial, and only

depend on the chosen value of  $N$ . Extending equation (B25) to a three-dimensional integral is straightforward.

In the software, a value of  $N = 20$  is chosen for each dimension of each integral, and this allows the integrated emissivity to be calculated in a few milliseconds to an accuracy of around 1 part in  $10^7$ . The values of  $x_i$  and  $w_i$  for  $N = 20$  are given in Table 1.

**Table 1.** Values of  $x_i$  and  $w_i$  for Gauss–Legendre integration with  $N = 20$ .

$i$	$x_i$	$w_i$
1	-0.993128599185095	0.0176140071391521
2	-0.963971927277914	0.0406014298003869
3	-0.912234428251326	0.0626720483341091
4	-0.839116971822219	0.0832767415767047
5	-0.746331906460151	0.10193011981724
6	-0.636053680726515	0.118194531961518
7	-0.510867001950827	0.131688638449177
8	-0.37370608871542	0.142096109318382
9	-0.227785851141645	0.149172986472604
10	-0.0765265211334973	0.152753387130726
11	0.0765265211334973	0.152753387130726
12	0.227785851141645	0.149172986472604
13	0.37370608871542	0.142096109318382
14	0.510867001950827	0.131688638449177
15	0.636053680726515	0.118194531961518
16	0.746331906460151	0.10193011981724
17	0.839116971822219	0.0832767415767047
18	0.912234428251326	0.0626720483341091
19	0.963971927277914	0.0406014298003869
20	0.993128599185095	0.0176140071391521

## References

- [1] MSL Technical Guide 22: "Calibration of low-temperature infrared thermometers", <http://msl.irl.cri.nz>.
- [2] MSL Technical Guide 26: "Size-of-source effect in infrared thermometers", <http://msl.irl.cri.nz>.
- [3] R E Bedford, C K Ma, "Emissivities of diffuse cavities: Isothermal and nonisothermal cones and cylinders", *Journal of the Optical Society of America*, **64**, 339–349, 1974.
- [4] R E Bedford, C K Ma, "Emissivities of diffuse cavities, II: Isothermal and nonisothermal cylindrical cones", *Journal of the Optical Society of America*, **65**, 565–572, 1975.
- [5] J V Nicholas, D R White, *Traceable Temperatures: An Introduction to Temperature Measurement and Calibration*, second edition, John Wiley & Sons, Chichester, 2001.
- [6] F E Nicodemus, "Emissivity of isothermal cavity with gray Lambertian walls", *Applied Optics*, **7**, 1359–1362, 1968.
- [7] P Saunders, D R White, "Physical basis of interpolation equations for radiation thermometry", *Metrologia*, **40**, 195–203, 2003.
- [8] R Siegel, J Howell, *Thermal Radiation Heat Transfer*, fourth edition, Taylor & Francis, New York, 2002.
- [9] S Chen, Z Chu, H Chen, "Precise calculation of the integrated emissivity of baffled blackbody cavities", *Metrologia*, **16**, 69–72, 1979.
- [10] W H Press, B R Flannery, S A Teukolsky, W T Vetterling, *Numerical Recipes*, Cambridge University Press, Cambridge, 1986.

*Prepared by Peter Saunders, December 2016.*